Available online at www.sciencedirect.com
SCIENCE DIRECT®
International Journal of Pharmaceutics 280 (2004) 77–93
international journal of pharmaceutics
www.elsevier.com/locate/ijpharm

# Interparticle van der Waals force in powder flowability and compactibility

Qin Li [a], Victor Rudolph [a,*], Bernhard Weigl [b], Alan Earl [c]

[a] *Chemical Engineering Division, University of Queensland, St Lucia, Brisbane, Qld 4072, Australia*
[b] *BASF AG GCT/T, Solids Handling, 67056 Ludwigshafen, Germany*
[c] *Herron Pharmaceuticals Pty. Ltd., Tennyson, Brisbane, Qld 4106, Australia*

Received 25 November 2003; received in revised form 17 March 2004; accepted 5 May 2004

**Abstract**

Particle flowability and compactibility are the two critical process parameters tested when a pharmaceutical material is formulated for a tabletting process. These behavioral descriptions are strongly affected by geometrical, physical, chemical and mechanical particle properties, as well as operational conditions. The property influences are broadly known in a qualitative sense, but have largely escaped fundamental quantitative description. Various measurement methods have been separately developed for each of these properties which provide comparative indices to assist in process and formulation design. This paper seeks to establish the connections between interparticle van der Waals force and both flowability and compactibility, and therefore also the inter-relations between the two apparently distinct properties. Paracetamol and the excipients often associated with it for tabletting are used as test materials to provide an initial validation of the theoretical development. These powders are well-characterized and known to be particularly difficult with respect to flowability and compactibility.


*Keywords:* Interparticle adhesion force; Van der Waals force; Flowability; Compactibility; Hausner ratio; Tablet strength

## 1. Introduction

The pharmaceutical industry relies on powder processing since more than 80% of its products are provided in tablet form (Jivraj et al., 2000). Pharmaceuticals have especially taxing quality requirements with regard to uniformity in content, consistency in appearance, longevity for storage, transportation and shelf life, demanding an exceptional degree of control and precision in their manufacture. Particle technologies require urgent improvement to meet these challenging requirements (Muzzio et al., 2002). An added complexity is that medicinal products are often blended mixtures of many different powders comprising active ingredients and various excipients for improving the dosage delivery and bioavailability. Among the many particle properties, flowability and compactibility are two essential characterizations to ensure a successful tabletting process (Guerin et al., 1999).

The flowability of a powder is a behavioral characterization of its ability to flow. Its vital importance in the production of pharmaceutical dosage forms is well-documented in the literature (Staniforth, 2002). Powder flowability is influenced by particle size, size distribution, shape, surface texture, surface energy, chemical composition, moisture content, vessel

* Corresponding author. Tel.: +61 7 3365 4171; fax: +61 7 3365 4199.
*E-mail address:* victorr@cheque.uq.edu.au (V. Rudolph).

0378-5173/$ – see front matter © 2004 Elsevier B.V. All rights reserved.
doi:10.1016/j.ijpharm.2004.05.001

**Nomenclature**

| | |
|---|---|
| $a$ | effective contact surface area |
| $a_{apparent}$ | apparent contact surface area |
| $a_p$ | potential effective surface area |
| $a'$ | contact surface area occurring in AFM measurement |
| $a_0$ | the radius of contact area between two spheres (JKR model) |
| $B$ | the total sectional area in a given sectional plane |
| $\bar{B}$ | the average sectional area of a particle in a given sectional plane |
| $d$ | particle diameter |
| $E$ | Young's modulus |
| $F_{AFM}$ | the pull-off force measured by AFM |
| $F_H$ | the adhesion force between two particles |
| $g$ | gravity acceleration constant |
| $k$ | mean coordination number |
| $m$ | the average number of particles cut by a sectional plane |
| $n$ | the number of bonds on a unit fracture plane |
| $r$ | radius of an asperity |
| $R$ | radius of a sphere |

*Greek Symbols*

| | |
|---|---|
| $\alpha$ | the adhesiveness, i.e., the adhesion force exhibited on a unit effective surface area |
| $\chi$ | geometry confinement |
| $\delta$ | yield stress |
| $\varepsilon$ | porosity |
| $\Phi$ | particle shape factor |
| $\gamma$ | the interfacial surface energy |
| $\varphi$ | volume fraction |
| $\mu$ | wall frictional property |
| $\nu$ | Poisson's ratio |
| $\rho$ | density |
| $\sigma$ | limited tensile stress; tablet strength |
| $\sigma_c$ | the applied stress |
| $\xi$ | deformation rate |
| $\psi$ | size distribution |
| $\zeta$ | fragmentation propensity |

geometry, and other factors. In response to this complexity, numerous methods for measuring powder flowability have been developed, largely based on empirical understanding. In practice, the measured results from these methods are not always consistent and may be hard to interpret. A common and easy method widely used in pharmaceutical industry for flowability measurement is the tapping test which provides Hausner ratio of the powder bed (Abdullah and Geldart, 1999). The value is obtained from the initial packing density (aerated density) and the final packing density after tapping in a controlled and defined way (tapped density). Correlations for tapping density with tapping number (Kawakita and Ludde, 1970; Yu and Hall, 1994) fail, however, to elucidate the underlying physics, or to satisfactorily explain the empirical observations.

Particle compactibility is defined as the ability of the powdered material to be compressed into a tablet of specified strength (Leuenberger, 1982). Pharmaceutical compacts are required to possess sufficient mechanical strength to withstand handling yet remain bioavailable. The mechanical strength of pharmaceutical compacts is characterized by the force required to fracture a specimen across its diameter, which is usually reported as "tablet hardness" in the pharmaceutical industry. The strength of a compact is a reflection of the bonding that has occurred during compaction. This relates to the type of bonds (a more complicated concept for a mixture), the number of effective bonds, contact surface area, and bond distribution in the compact. Since virtually all tablets consist of more than one material, the prediction of the compaction properties of mixtures from those of the individual components is of obvious interest (van Veen et al., 2000). Most investigations in this area are limited to binary mixtures and are directed at the relation between tablet strength and the relative proportions of the components. Nevertheless, a single unified theory to account for the compaction of binary mixtures is not yet available.

Both flowability and compactibility are functionally dependent on the interparticle attraction (Fuhrer, 1996). Interparticle adhesion is caused by intermolecular forces including van der Waals forces, local chemical bonds, electrostatic charges, and bridging forces, mainly surface liquid capillary attractions. These forces are strongly affected by surface properties such as texture, surface chemistry, adsorption

layers, and contact area. For larger particles, gravity and inertia are generally greater than the interparticle adhesion force, hence they normally flow easily. For fine particles (less than ~10 μm), the interparticle adhesion force is appreciable relative to gravity. Therefore, they tend to adhere to one another and are problematic to handle. Quantifying these interactions is a complicated problem with the many entwined variables. In compaction, the dominating interparticle bond types are identified as solid bridges, intermolecular forces as above, and mechanical interlocking. The predominant interaction force between solid surfaces is the van der Waals force (Derjaguin et al., 1956). Hiestand (1985) developed theoretical models for predicting tablet tensile strength considering interparticle dispersion forces and deformation, later including viscoelastic properties (Hiestand, 1991).

Various excipients are added in tablet formulations acting as binders, lubricants and disintegerants in order to improve the processability and bioavailability of the tablet product, often through granulation processes. However, direct compaction without granulation, is gaining interest as alternative means of changing particle properties become available (Bolhuis and Chowhan, 1996). The economic drive for direct compaction is the reduced number of operation units, and quality improvement when the active ingredient is heat and moisture sensitive. On the other hand, direct compaction requires high flowability and compactibility of the constituent ingredients, to assure the quality of each individual tablet. Paracetamol tabletting is a good example which has a long history of research (Martino et al., 1996; Garekani et al., 2000; Beyer et al., 2001) seeking appropriate modifications to the pure Paracetamol crystals, which are notorious for poor flowability, and compactibility, and for being difficult for direct compaction. Typical excipients which normally comprise about 10% (w/w) are added in the commercial manufacture of Paracetamol tablets.

This paper explores (1) the measurement and data interpretation of interparticle pull-off forces, (2) the influence of the interparticle van der Waals force on powder flowability, (3) the influence of the interparticle van der Waals force on mechanical strength of the compacted body, and (4) the relationship between flowability and compactibility. Both theoretical analysis and experimental examination were carried out. Various measurements on different scales were conducted in the attempt to link the particles' microscopic properties with their bulk characteristics. Materials and ingredients typically used for Paracetamol tabletting process form the basis of the experiments.

## 2. Materials and methods

### 2.1. Materials

The test materials consist of six pharmaceutical powders, which were provided by Herron Pharmaceuticals Pty. Ltd. Among them, Paracetamol is the active ingredient in its pure crystalline form. The rest namely Povidone, Crospovidone, Pregelatinised Starch, Stearic Acid, and Magnesium Stearate are common pharmaceutical excipients. The descriptions of their major properties and functions in tabletting can be found in the Handbook of Pharmaceutical Excipients (Kibbe, 2000).

The particle sizes and microscopic morphology for each type of material were obtained through Malvern Autosizer 2600C and SEM, respectively. The particle sizes measured by the dry method are presented in Table 1. The SEM images of Paracetamol are shown in Fig. 1 and for Preglatinised Starch in Fig. 2, while the rest can be found in the handbook (Kibbe, 2000).

In Table 1, the span is a measure of the distribution of the particle size:

$$\text{Span} = \frac{D_{90\%} - D_{10\%}}{D_{50\%}} \quad (1)$$

where, $D_{90\%}$ is the diameter ($D_{4,3}$) for which 90% of the sample is smaller, $D_{50\%}$ is the diameter ($D_{4,3}$) for which 50% of the sample is smaller, i.e. the median diameter. $D_{10\%}$ is the diameter ($D_{4,3}$) for which 10% of the sample is smaller.

### 2.2. Methods

#### 2.2.1. Particle-level

*2.2.1.1. Pull-off force measurement.* The atomic force microscopy (AFM) presents a method to measure the release forces of the particles in the range from $10^{-6}$ to $10^{-12}$ N. The mechanism of AFM is illustrated by Fig. 3. One particle is attached to the cantilever of the AFM, another to a piezo crystal element which forms the test particle base. The position

Table 1
Particle size

| Material | $D_{4,3}$[a] (μm) | $D_{3,2}$[b] (μm) | $D_{90\%}$ (μm) | $D_{10\%}$ (μm) | $D_{50\%}$ (μm) | Span |
|---|---|---|---|---|---|---|
| Paracetamol | 285 | 71 | 538 | 30 | 253 | 2.01 |
| Povidone | 150 | 80 | 266 | 44 | 134 | 1.66 |
| Crospovidone | 178 | 78 | 360 | 38 | 143 | 2.25 |
| Pregelatinised Starch | 96 | 45 | 175 | 19 | 86 | 1.80 |
| Magnesium Stearate | 10 | 7.3 | 21 | 4.7 | 6.5 | 2.56 |
| Stearic Acid | 119 | 81 | 220 | 45 | 102 | 1.72 |

[a] $D_{4,3}$ is the volume or mass moment mean: $D_{4,3} = \sum_n d_n^4 / \sum_n d_n^3$.
[b] $D_{3,2}$ is the surface area moment mean: $D_{3,2} = \sum_n d_n^3 / \sum_n d_n^2$.

when the two particles are in contact for the first time is registered to the computer. The cantilever is retracted from the test particle base and the adhesion forces between the particles are measured as a deflection of the cantilever. The spring constant of the cantilever was obtained by the thermal noise method. The particle–particle contact time is 1 s during the measurement as the frequency was set as 1 Hz. The relative humidity was kept constant between 45 and 50%. Each set of tests was done 100 times by us-

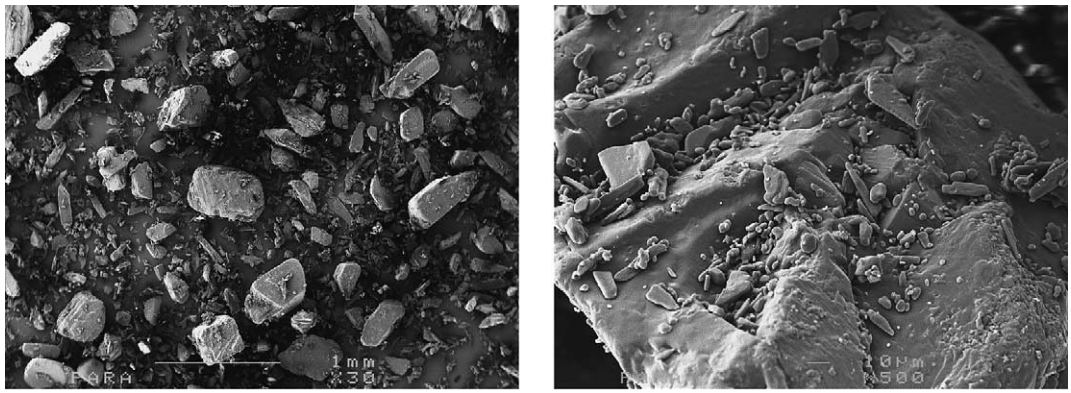


(a) (b)

Fig. 1. SEM images of (a) Paracetamol particles and (b) a particle surface.

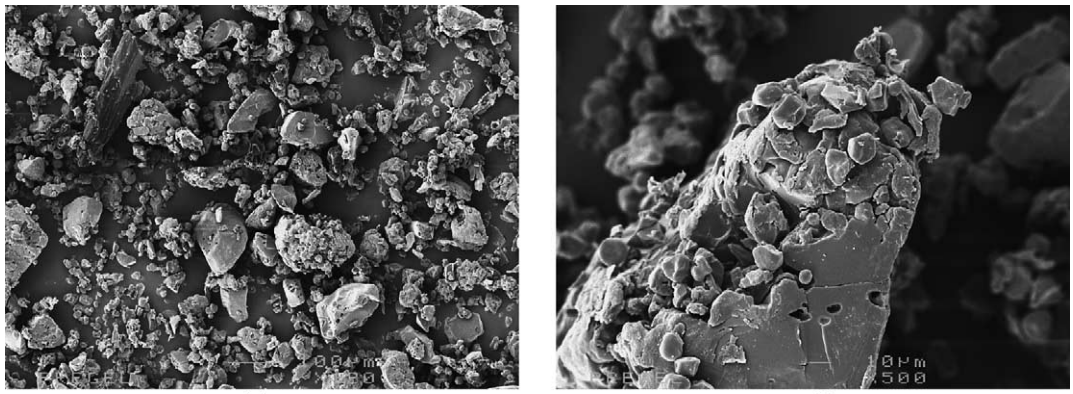


(a) (b)

Fig. 2. SEM images of (a) Pregelatinised Starch particles and (b) a particle surface.

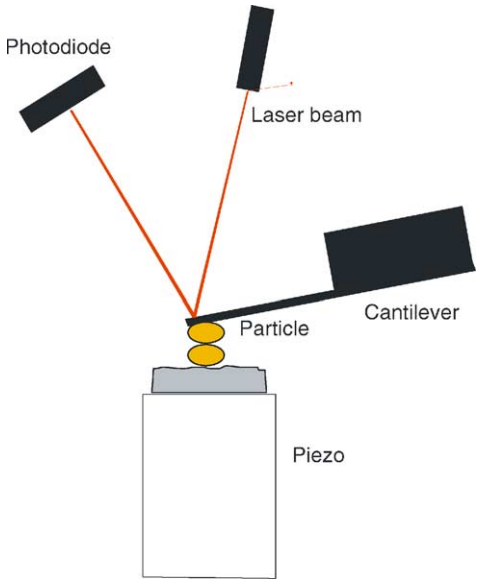


Fig. 3. An illustration of the mechanism in AFM measurement.

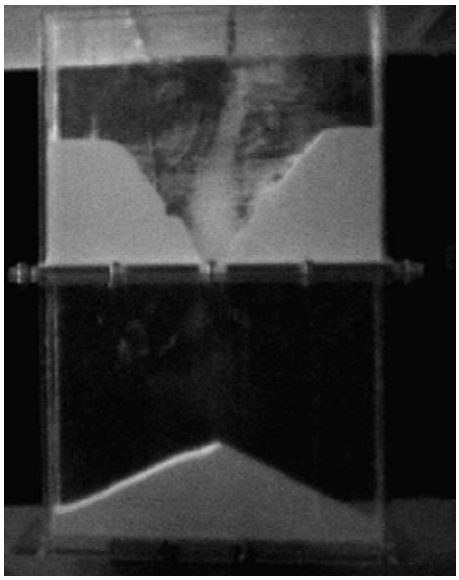

Fig. 4. The bin-flow tester.

ing 20 different pairs of particles with 5 repetitive measurements for each pair.

*2.2.1.2. Tapping density test.* The densities of bulk and settled powders provide the Hausner ratio (HR):

$$\mathrm{HR} = \frac{\mathrm{density}_{\mathrm{tapped}}}{\mathrm{density}_{\mathrm{aerated}}} \quad (2)$$

A Quantachrome dual autotap machine and two 50 ml graduated measuring cylinders were used in this test. The cylinder was filled with the desired mass of powder. The initial volume was recorded and the poured density was calculated. After 10, 250, 500, 1250 and 2000 taps the corresponding volume was read to the nearest milliliter. When the difference between the two volumes was smaller than 1ml and 2%, the tapped volume was recorded. For Povidone, Crospovidone, $V_{500}$ was used. For 100% Paracetamol, Pregelatinised Starch, and Stearic Acid, $V_{1250}$ was used. For Magnesium Stearate $V_{2000}$ was used.

*2.2.1.3. Bin-flow test.* A specific device resembling the design of Zenz and Othmer's early work (Zenz and Othmer, 1960) is used to manifest particles' flow behavior as shown in Fig. 4. The top and bottom chambers, which are separated by a dividing plate, are geometrically identical: 250 mm (width) × 20 mm (thickness) × 200 mm (height). In the middle of the divider is a square opening (20 mm × 20 mm), which can be shut and opened by a metal slide. The whole apparatus can be placed on the Quantachrome tapping machine, e.g. when the powder is cohesive and requires assistance to flow. When powder flow is initiated, a medium speed camera and image acquisition software are triggered to continuously photograph the system at 10 Hz. The angle of drain, poured angle of repose, the required external energy, and the instantaneous and cumulative powder mass flow are obtained simultaneously. The bin-flow test provides a 'reality-check' for particle flowability.

*2.2.2. Tablet-level*

*2.2.2.1. Tablet preparation.* Sample tablets of 600 ± 20 mg were compacted using a rotary tablet press (Betapress, Manesty) with beveled edged 12 mm diameter punches. The lower punch face was grooved whilst the upper punch was flat-faced. For all materials the punch and die height was kept constant and the force was kept at 2 t. Tablets made from each component individually as well as binary sample mixtures containing 90% pure Paracetamol and 10% of each excipient (by mass), were produced. For the mixtures, homogeneity was achieved by shaking the weighed amounts in mixing bags for 5 min each, prior to compaction. Im-

mediately after compaction the tablets were weighed to ensure they were within the specified mass limits. The tablets were stored in plastic containers at a temperature of 23 °C and 55% humidity for 4 days.

*2.2.2.2. Diametrical compression.* Diametrical compression testing is widely used in pharmaceutical industry to measure the mechanical strength of tablets. The force required to fracture a specimen across its diameter is reported as the 'hardness value'. This terminology is potentially confusing compared with the more precise definition of hardness as used in material science associated with indentation (Davies and Newton, 1996), and tablet 'mechanical strength' is a better term in this context. In this work, a Schleuniger-2E 'hardness' tester was used. The sensitivity and accuracy of this equipment is not ideal; if the applied force is less than 0.6 kPa, there is no reading.

## 3. Results and discussions

### 3.1. Measured interparticle adhesion force

The AFM measurements were performed on all pair combinations for the six materials. Each combination was measured 100 times (made up of 20 distinct particle pairs, each pair measured five times). There are different ways to select the representative values of the adhesion forces, and some difficulties in understanding the statistical significance of the measured adhesion force value (Gotzinger and Peukert, 2003). For

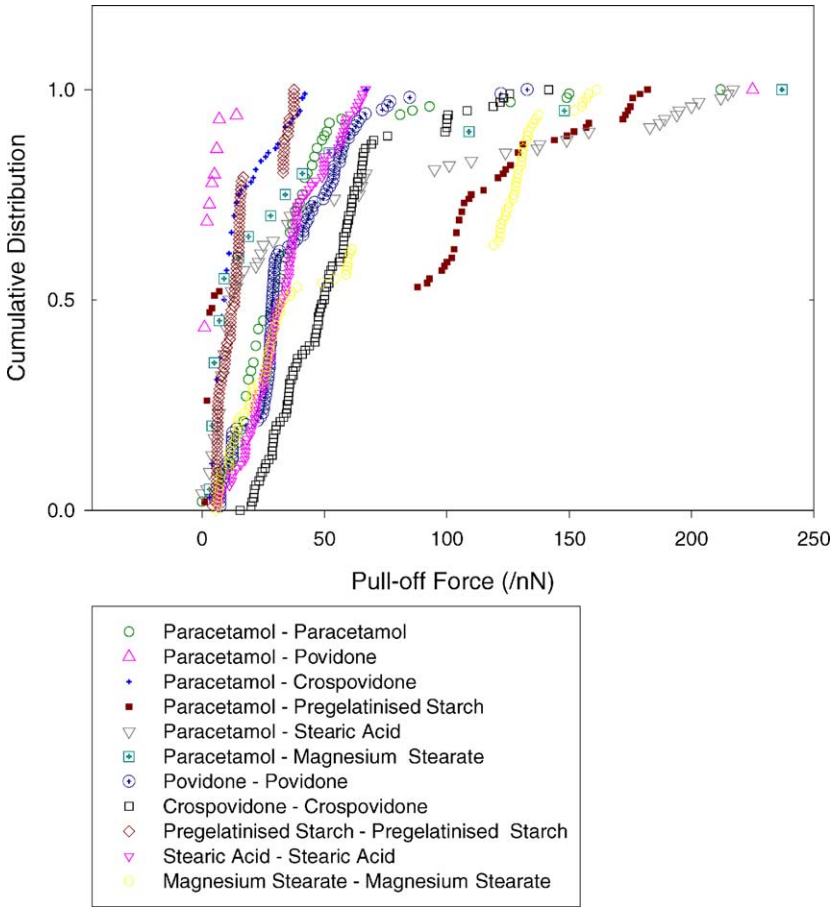


Fig. 5. Cumulative distribution vs. pull-off force for particle–particle interfaces.

Table 2
The average values of interparticle van der Waals force among the powders

| Particle pair | Mean adhesion force (nN) | Standard deviation (nN) | Median adhesion force (nN) | Span |
|---|---|---|---|---|
| Paracetamol–Paracetamol | *35* | *31* | *30* | *1.31* |
| Paracetamol–Povidone | 16 | 53 | 1.2 | 3.00 |
| Paracetamol–Crospovidone | 14 | 12 | 9.0 | 3.22 |
| Paracetamol–Pregelatinised Starch | 62 | 65 | 5.0 | 30.1 |
| Paracetamol–Stearic Acid | 47 | 64 | 11 | 14.09 |
| Paracetamol–Magnesium Stearate | 37 | 60 | 10 | 13.19 |
| Povidone–Povidone | *36* | *22* | *29* | *1.79* |
| Crospovidone–Crospovidone | *53* | *26* | *50* | *1.46* |
| Pregelatinised Stach–Pregelatinised Starch | *16* | *11* | *13* | *2.23* |
| Stearic Acid–Stearic Acid | *34* | *15* | *33* | *1.32* |
| Magnesium Stearate–Magnesium Stearate | *66* | *54* | *33* | *3.67* |

very spherical particles, the force of the maximum occurrence is often taken as the detachment force, with other values assumed due to measurement inaccuracies and deformations of the particles or the surface during the measurements. However, in this work, the particles have very irregular shapes, rough surfaces and other variant properties, contributing to a very broad data spread as presented in Fig. 5. This corresponds with literature reports (Beach et al., 2002) that roughness of the interacting surfaces is the significant factor affecting experimentally measured pull-off forces. Further, the size, shape, orientation and surface condition vary among the 20 pairs of particles for each set of measurements. Even the five repetitions for the same particle pairs showed significant variability in the measured values. The broad distribution of pull-off force values is attributed to the changes in the adhesive contact area. Table 2 presents the mean adhesion values and standard deviations based on the experimental measurements, along with the 50% median value and the span. Median values are most commonly used in the literature (Podczeck et al., 1997; Quintanilla et al., 2001; Beach et al., 2002) and have been used here also as the representative value for further analysis.

The adhesion forces measured here are considered only to be the van der Waals force. This is justified as the particles were kept dry before the measurements, thereby eliminating surface liquid capillary attraction; the contact time is only 1 s which is too short for the formation of local chemical bonds or solid bridges; the chamber relative humidity of 40–50% is sufficient to allow dissipation of any static charges and eliminates the possibility of significant electric-static force.

In this section we focus on the cohesion force between single material particle pairs as italicized in Table 2. Fig. 5 shows the cumulative distributions of measured adhesion forces between all the particle pairs. Some speculations, based on the experimental observations are addressed in the following.

### *3.1.1. Paracetamol*

The curve of Paracetamol–Paracetamol in Fig. 5 shows the cohesion forces between Paracetamol particle pairs vary from almost 0 to 230 nN. SEM images in Fig. 1 demonstrate that the Paracetamol particles have an extremely wide size distribution (evidenced also by the size distribution span value, 2.01, Table 1), block/needle shape, and rough surfaces. The wide spread of adhesion force is most probably caused by the size distribution, irregular shape, and the orientation of the particles. For each pair of Paracetamol particles, the contact surface area may vary extensively due to these uncontrolled factors.

### *3.1.2. Povidone*

Despite the mild span of size distribution, 1.66, the adhesion force of Povidone has a relatively wide spread of 1.79. The SEM image (Kibbe, 2000) suggests that the spherical part of a Povidone particle has a very smooth surface. The cumulative curve of adhesion force on Fig. 5 illustrates that 40% of the measurements show an interparticle force around 30 nN and 20% are around 15 nN. The higher adhesion force measurements, which occur more rarely, are possibly caused by the hollow part of the particle inducing mechanical locking between the particles.

*3.1.3. Crospovidone*

In contrast to Povidone, Crospovidone provided a measured size distribution with a very broad span, 2.3, Table 1, but the adhesion force, with a span value of 1.46, has a smaller spread. The cumulative curve of adhesion force demonstrates an even distribution with 85% of the measurements ranging from 20 to 70 nN. The small number exhibiting very high adhesion force may be due to two large surfaces in contact, or the occurrence of mechanical interlocking because of its porous structure shown in the SEM image (Kibbe, 2000). On average, Crospovidone has a rather high adhesion force compared with the other materials.

*3.1.4. Pregelatinised Starch*

The angular-shaped Pregelatinised Starch particles have a moderate size distribution span of 1.80. The SEM images, Fig. 2, show an irregular particle surface often having holes or steps and with smaller particles on the surface. A bimodal distribution of the adhesion force is clearly shown in Fig. 5. About 80% of Pregelatinised Starch particle pairs have adhesion force evenly distributed around 15 nN, and another 20% fall around 45 nN. The span value in this case, 2.23, is misleading because it suggests a very broad spread, disguising the bimodal distribution. The reason for the bimodal adhesion distribution is not clear. Possibly, around 80% of the contact surface is rather smooth and 20% of the surface is irregular and rough. Nevertheless, in an overall sense, Pregelatinised Starch can still be categorized as non-cohesive powder based on this AFM result.

*3.1.5. Stearic Acid*

The size distribution of Stearic Acid is moderately broad. The particles have irregular angular shape and display a tendency to agglomerate. It was found that the particles are easily charged during the SEM imaging process. The pull-off forces are quite evenly distributed, shown in Fig. 5, with small groupings at around 30 nN and around 55 nN.

*3.1.6. Magnesium Stearate*

It is a very fine powder extremely prone to agglomerate. The mean size from Malvern Autosizer 2600 is about 10 μm; however, the size distribution curve shows bimodal or even tri-modal tendencies, a result of agglomeration. Therefore, the real individual particle size may be expected to be below 10 μm. As shown in SEM image (Kibbe, 2000), although the particles are agglomerated, the individual particles are identifiable, being very fine with a platelet shape and flaky structure. This size and shape supports strong adhesion because the van der Waals force easily exceeds the gravity force on a particle. These issues present problems for the AFM measurements, because it is impossible at this stage to make measurements on an individual Magnesium Stearate particle. The adhesion force measured between Magnesium Stearate and Magnesium Stearate is actually the adhesion force between two layers of particles. The adhesion force obtained between Magnesium Stearate and Paracetamol is actually between a layer of Magnesium Stearate and a Paracetamol particle surface with adhered Magnesium Stearate powders. Hence, the AFM results for particle pairs involving Magnesium Stearate as a material provide some reference data, but cannot be considered comparable to the other particle interaction measurements.

*3.2. Theoretical interpretation on AFM results*

The AFM measurements and SEM visualizations suggest multiple-contact points during the measurement. The interpretation of these results is discussed in this section.

There are several forms of developed interparticle adhesion models calculating van der Waals force including: Hamaker integration, further developed to take into account the surface roughness by Rumpf (1990) and Rabinovich et al. (2000a, 2000b); Krupp's model using Lifschitz–van der Waals constant (Krupp, 1967); and JKR model based on Hertzian theory (Johnson et al., 1971).

The Rabinovich model is widely regarded as the most accurate for materials with rough surfaces. However, it has serious limitation that it assumes no local deformation, which makes it unsuitable for many pharmaceutical powders. For example, Beach et al. (2002) showed that adhesion between peptide materials and polystyrene measured by AFM is an order of magnitude higher than the model estimates, and attributed this differences to particle deformation.

Here, we propose a model combining JKR model with the roughness concept embedded in Rumpf–Rabinovich model. The concept is illustrated

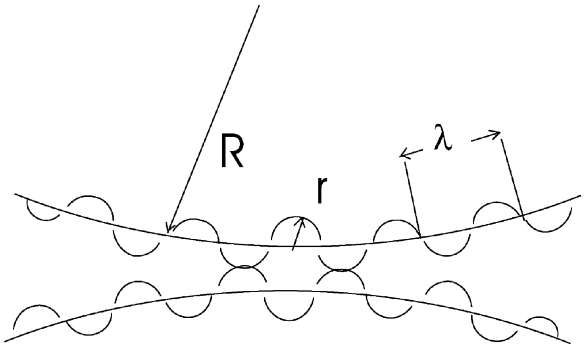


Fig. 6. A schematic drawing of two rough-surfaced particles in contact.

in the schematic drawing, Fig. 6. We postulate that the adhesion force between two particles is determined by its adhesiveness $\alpha$, and the effective contact surface area $a$:

$$F = \alpha a \tag{3}$$

The adhesiveness $\alpha$ is defined as the adhesion force exhibited on a unit effective surface area. When two surfaces are in contact, it is the asperities on the surface that are in real contact. We apply JKR model, on the asperities whose radius is $r$, to obtain $\alpha$:

$$\alpha = \frac{3\pi r\gamma}{\pi a_0^2} \tag{4}$$

where $\gamma$ is the interfacial surface energy and $a_0$ is the contact radius under zero load calculated by Hertzian theory, $a_0 = \sqrt[3]{18\pi\gamma r^2(1-\nu^2)/E}$; $\nu$ is Poisson's ratio and $E$ is Young's modulus. One of the conditions to apply JKR theory is that the characteristic radius of the contact area, arising from deformation of the asperity, needs to be much smaller than the sphere radius (of the asperity). The difference for the particles used in this study is generally about two orders of magnitude. Typical dimensions of the asperities at different measuring scales have been reported by Beach et al. (2002).

Substituting $a_0$ into Eq. (4) gives,

$$\alpha = \frac{1}{\sqrt[3]{12\pi^2 r(1-\nu^2)^2/E^2}}\gamma^{1/3} \tag{5}$$

This expression clearly shows that the surface adhesiveness, $\alpha$, is an inherent material property of the particle determined by its surface energy, surface roughness, Young's modulus and Poisson's ratio.

At a particle level, the apparent contact area between particles encompasses many asperities, that is, if $a_{\text{apparent}}$ denotes the observable macroscopic contact surface area then its characteristic radius $\gg r$. Assuming the statistical distribution of asperity peaks and valleys are the same, then the potential effective contact surface area is:

$$a_{\text{p}} = \frac{1}{2}a_{\text{apparent}} \tag{6}$$

The effective contact surface area is:

$$a = a_{\text{p}}\frac{\pi a_0^2}{\pi r^2} = \frac{3\sqrt[3]{12\pi^2\gamma^2 r(1-\nu^2)^2/E^2}}{2r}a_{\text{apparent}} \tag{7}$$

For an interface consisting two different materials, the effective contact surface area depends on the nature of the materials.

Because the ratio between the effective contact area and the apparent contact area is a constant for the certain type of material, we simply refer to the effective contact area only in the following discussion for convenience.

When two rough surfaces of irregular shaped particles are in contact, the measured adhesion force by AFM can be expressed as:

$$F_{\text{AFM}} = \alpha a' \tag{8}$$

Currently, there is no way to experimentally determine the contact surface area $a'$. However, the measured adhesion force by AFM, $F_{\text{AFM}}$, itself can be considered as a reference when the contact adhesion forces under various conditions are discussed:

$$F = \alpha a = (\alpha a')\frac{a}{a'} = F_{\text{AFM}}\frac{a}{a'} \tag{9}$$

If the particles are compressed under pressure, $a/a'$ can be estimated by a correlation between the applied stress $\sigma_{\text{c}}$, the pull-off force $F_{\text{AFM}}$, and other particle mechanical properties. When the compression is within the elastic deformation regime, the ratio is:

$$\frac{a}{a'} = \frac{\sigma_{\text{c}}}{F_{\text{AFM}}} \tag{10}$$

Otherwise, the viscoelastic property of the material has to be identified and the ratio between $a$ and $a'$ is more complicated.

Table 3
The comparison of flowability derived from Hausner ratios and bin-flow tests

| Material | Aerated density (g/ml) | Tapped density (g/ml) | HR | Flowability according to HR | Flowability according to bin-flow test | Particle size, $D_{4,3}$ (μm) | Median adhesion force (nN) |
|---|---|---|---|---|---|---|---|
| Povidone | 0.384 | 0.434 | 1.13 | Good | Good | 150 | 29 |
| Crospovidone | 0.337 | 0.345 | 1.02 | Good | Poor | 178 | 50 |
| Pregelatinised Starch | 0.629 | 0.784 | 1.25 | Poor | Fair | 96 | 13 |
| Stearic Acid | 0.391 | 0.496 | 1.27 | Poor | Very poor | 119 | 33 |
| Paracetamol | 0.602 | 0.834 | 1.39 | Very poor | Very poor | 285 | 30 |
| Magnesium Stearate | 0.289 | 0.401 | 1.39 | Very poor | Very poor | 10 | 33 |

### 3.3. Hausner ratio and adhesion force

Tapping tests were carried out for each of the six materials. From the aerated and tapped densities, Hausner ratios were calculated for the respective powders as shown in Table 3. The aerated bulk density of a powder is determined by allowing the dispersed powder to settle in a container under the influence of gravity. A powder with a strong structural strength will resist collapse when dispersed in a container and will have a low bulk density, while a structurally weak powder will collapse easily and have a high bulk density. The tapped bulk density is obtained by tapping the container holding the aerated sample. The structure of a cohesive powder will collapse significantly on tapping while the weak or free-flowing powder has little scope for further consolidation. Hausner ratio as a characterization property is developed based on this theory, connected to practically important handling features by some general rules (Geldart et al., 1984; Geldart and Wong, 1984; Yu and Hall, 1994).

According to these rules, the Hausner ratios from our tapping tests show that Povidone and Crospovidone have very good flow property, Pregelatinised Starch and Stearic Acid have poor flowability, whilst Paracetamol and Magnesium Stearate have very poor flowability (Table 3).

To examine whether Hausner ratios have provided the correct characterizations, bin-flow tests were carried out for comparison and the results are also presented in Table 3. It is noticeable that there are two serious discrepancies and another minor one: Crospovidone flows very poorly in reality instead of possessing ‘good’ flowability as Haunser ratio suggests; Pregelatinised Starch has a reasonably good flowability in the bin test, not ‘poor’ as deduced from Hausner ratio; Stearic Acid is much worse than the ‘poor’ flowability characterization from the Hausner ratio. Similar discrepancies between Hausner ratio results in comparison with real flow situations are reported, e.g. in Schussele and Bauer-Brandl (2003) and elsewhere.

For a powder like Crospovidone possessing high surface cohesiveness, tapping does not seem to result in significant volume reduction. There are two possible explanations: (a) because the material is so cohesive, and the particles have a reasonable sphericity, the initial aerated density is already quite tightly packed and there is little room for rearrangement. In addition, the particles are rather hard so consolidation due to local deformation cannot occur; (b) because of the high cohesiveness of the powder, the energy supplied by the tapping machine is insufficient to break the initial structure and to allow further rearrangements of the particles. The latter hypothesis is supported by some literature (Abdullah and Geldart, 1999) reporting that more vigorous tapping using a Hosokawa Powder Tester provided ‘accurate measurement’ due to the significant increase of tapping intensity. Both the conventional tapping machine and Hosokawa Powder Tester have an output speed of 250 rpm, but the cam of Hosokawa Powder Tester raises the cylinder platform through a distance of 25 mm compared with 3 mm for the conventional ones.

For a powder like Pregelatinised Starch, having an almost bimodal (or tri-modal) size distribution, an irregular angular shape, and a rather non-cohesive surface, tapping can result in a significant volume reduction, because it allows the particles to reorient. The smaller particles then have opportunities to find interstitial spaces within the coarser material. Since the interparticle cohesive forces are low, this behavior does not necessarily lead to poor flowability.

To analyze the problem theoretically, in a random packed bed with a hypothetical state of isostatic stress, the limiting tensile stress, $\sigma$, is (Rumpf, 1970):

$$\sigma = \frac{1-\varepsilon}{\varepsilon}\frac{F_H}{d^2} \tag{11}$$

where $F_H$ denotes the adhesion force existing at a single interparticle contact, $\varepsilon$ is the bed porosity, and $d$ denotes the particle diameter. With uniform random packing of equal sized spheres, the average sectional area of a particle in a given sectional plane is $\bar{B} = (\pi/6)d^2$ (Molerus, 1982), the average number $m$ of particles cut by the sectional plane then is calculated from $m(\pi d^2/6) = (1-\varepsilon)B$, where $B$ is the total sectional area. Therefore, the average limiting tensile force transmitted per particle in a bed of porosity $\varepsilon$ is (Rumpf, 1970):

$$F_T = \frac{\sigma B}{m} = \frac{\pi}{6}\frac{F_H}{\varepsilon} \tag{12}$$

Substituting $F_H$ with Eq. (3), gives:

$$F_T = \frac{\pi}{6}\frac{\alpha a}{\varepsilon} \tag{13}$$

where the average interparticle contact surface area $a$ depends on particle and vessel properties. It is a function of particle size $d$, size distribution $\Psi$, shape characterized as shape factor $\phi$, surface energy $\gamma$, and surface roughness $r$. It is also determined by the stress distribution within the powder body due to the geometrical confinement $\chi$ and wall frictional property $\mu$ of the vessel, and the gravity force of the particle $\rho_{\text{particle}}d^3g$. Further it depends on the mechanical properties of the particle: Young's Modulus $E$, yield stress $\delta$, deformation rate $\xi$, fragmentation propensity $\zeta$. If we consider the powder body is free from other externally applied stress, then $a$ can be expressed as $a(d, \psi, \phi, \gamma, r, \chi, \mu, \rho_{\text{particle}}d^3g, E, \delta, \xi, \zeta)$. The packing porosity $\varepsilon$, is also a function of the same set of variables, hence, expressed as $\varepsilon(d, \psi, \phi, \gamma, r, \chi, \mu, \rho_{\text{particle}}d^3g, E, \delta, \xi, \zeta)$. A more detailed analysis on these correlations is to be developed in future work.

When the particles flow without external assistance, it is the gravity force that counterbalances the strength of the powder body. Thus, a particle flowability criterion can be derived as Eq. (14). Combined with Eq. (5) the flowability criterion is completely expressed using only the fundamental properties of the powder. In this context, the flowability has become independent of the operational device geometry:

$$\rho_{\text{particle}}d^3g \geq \frac{\alpha a}{\varepsilon} = \frac{\gamma^{1/3}}{\sqrt[3]{12\pi^2 r(1-\nu^2)^2/E^2}}\frac{a}{\varepsilon} \tag{14}$$

where $\rho_{\text{particle}}$ is the particle density, $g$ is the gravity acceleration constant. We can also rearrange the criterion so that it can be expressed using the experimentally measurable value $F_{\text{AFM}}$

$$\rho_{\text{particle}}d^3g \geq \frac{F_{\text{AFM}}}{\varepsilon}\frac{a}{a'} \tag{15}$$

The mechanism of tapping test relates to breaking the existing interparticle bonds to allow particles to rearrange their positions and to permit the smaller particles to find voids. The volume reduction rate is an indication of the strength of the original packing: the higher the rate, usually the higher the original strength. However, it is important to note that in order to break interparticle bonds, the force exerted via tapping has to be greater than the limiting tensile force, which is proportional to particle adhesiveness $\alpha$, and contact surface area $a$, and is inversely proportional to the packing porosity $\varepsilon$.

The well-discussed influences of particle size and shape on the value of Hausner ratio are clearly shown in Eq. (14). The cubic power relationship of the particle size confirms the extreme sensitivity of particle flowability to the size. Particle size and shape also influence the contact surface area $a$. The smaller the particles, the broader the size distribution, and the more angular the particle shape, the larger is contact surface area $a$. Therefore, the limiting tensile stress is higher and the powder appears less able to flow. Eq. (14) quantitatively demonstrates how the particle density, adhesiveness, $\alpha$, and the packing porosity, $\varepsilon$, affect the powder flowability.

Based on this theory, the two hypothetical explanations offered earlier are both valid in the case of Crospovidone. In the case of Pregelatinised Starch, because of the very wide size distribution and irregular angular shape, the interparticle contact surface is relatively large. At the initial status, it formed a loose structure with many voids. However, it is a very weak structure because the powder has a low interparticle adhesion force, evidenced by the measured AFM pull-off force. Once this structure is shaken off, the particles start to flow and once flowing, it is difficult

to stabilize at another weak structure. Therefore, it is flowable despite the high Hausner ratio.

### 3.4. Tablet strength and adhesion force

It is argued that van der Waals force, or more specifically, the dispersion force is the major bonding force, which determines the tablet strength in pharmaceutical compacts, along with several other parameters (Hiestand, 1985, 1991). In a simplistic way, the interparticle bond strength is assumed to be directly proportional to the tablet strength. The interparticle bond strength $F_H$, is directly proportional to contact area $a$, and particle–particle adhesiveness $\alpha$.

In the compaction process, the influences of the particle mechanical properties: Young's modulus $E$, yield stress $\delta$, deformation rate $\xi$, and fragmentation propensity $\zeta$, as well as the externally applied stress $\sigma_c$, become much more important than in the particle flow condition, because significant contact deformation and fragmentation alter the interparticle contact surface area.

Nevertheless, the tablet strength $\sigma$, can still be described with a simple equation involving the mean bond strength and the number of bonds $n$, on a unit fracture plane:

$$\sigma = nF_H \tag{16}$$

Substituting $F_H$ with Eq. (3), we obtain:

$$\sigma = n\alpha a \tag{17}$$

Referring to Eq. (10), Eq. (17) can be further rearranged as:

$$\sigma = F_{AFM} n \frac{a}{a'} \tag{18}$$

Thus, tablet strength is shown to be directly proportional to the surface adhesiveness $\alpha$, number of contacts on a unit fracture plane $n$, and the average contact area $a$. It should also be in linear relationship with measured adhesion force by AFM when $a/a'$ is a constant.

The mechanical strength value obtained from diametrical compression testing is much more complicated because the fracture plane is caused by crack propagation. In an ideal situation, if all the particles in a tablet are spherical, of the same kind, and perfectly aligned, under diametrical compression the tablet will fracture into two perfect halves if it is made of brittle material, or deform into an ellipsoidal shape if it consists of ductile material. But in reality, the fracture propagates from the weakest point—a defect in the structure that concentrates the stress and causes a crack to propagate. Thus, particle size, size distribution, particle shape, adhesiveness, elasticity, plasticity, and fragmentation propensity are all important contributors to the final tablet strength. Under different circumstances, different variables dominate.

Most literature addressing tablet strength restrict the discussions around original particle size, shape, and compression pressure (Alderborn, 1996). Not much attention has been paid to the influence of interparticle adhesions. Rumpf (1962) developed an expression Eq. (19) for the strength of an aggregate of monodispersed spheres based on considerations of bonding force at contacts for loosely packed beds of particles. This equation is equivalent to Eq. (11):

$$\sigma = \frac{9(1-\varepsilon)kF_H}{8\pi d^2} \tag{19}$$

where $\varepsilon$ is the porosity of aggregate, $k$ is the mean coordination number. Hiestand derived a set of tensile strength models taking into account the microscopic properties (Hiestand, 1991). However, the usage of the hardness and strain indexes makes the models less than straightforward, because the underlying physical meaning of these values is not known.

For a tablet made of binary mixtures, there are three co-existing types of bonds, namely A–A, B–B, A–B. It seems reasonable to assume that the tablet strength is determined by the distribution of the weakest bonds in the system.

Ten kinds of tablet samples were made: Paracetamol, Crospovidone, Povidone, Pregelatinised Starch, Stearic Acid, Paracetamol–Crospovidone, Paracetamol–Magnesium Stearate, Paracetamol–Povidone, Paracetamol–Pregelatinised Starch, Paracetamol–Stearic Acid. In the binary-mixture tablets, Paracetamol always weighs 90% (w/w). Magnesium Stearate could not be made into tablet form in its own right.

Table 4 is a summary of various properties of the tablets that were made. The appearances of the tablets differ a great deal: some of them appear very friable and weak while some of them have smooth surfaces and appear as solid compacts. The porosities reported

Table 4
The tablet strength and the measured interparticle adhesion forces

| Tablet | Appearance | Porosity | Median adhesion force (nN) | Measured strength (kPa) | Hypothetical strength based on Rumpf's theory (Pa) |
|---|---|---|---|---|---|
| Paracetamol | Very friable, easy to chip off | 0.21 | 30 | 2.03 | 0.49 |
| Povidone | Smooth surface, solid compact | 0.15 | 29 | 18.13 | 1.29 |
| Crospovidone | Friable, solid compact | 0.15 | 50 | 3.98 | 1.59 |
| Pregelatinised Starch | Extremely friable, very loose compact | 0.18 | 13 | 0.90 | 1.66 |
| Stearic Acid | Smooth surface with defects, solid compact | 0.14 | 33 | 2.86 | 2.21 |
| Paracetamol–Povidone | Very friable, loose compact | 0.35 | 1.2 | 0* | 0.03 |
| Paracetamol–Crospovidone | Very friable, loose compact | 0.19 | 9.0 | 0.8 | 0.15 |
| Paracetamol–Pregelatinised Starch | Extremely friable, loose compact | 0.28 | 5.0 | 0.78 | 0.12 |
| Paracetamol–Stearic Acid | Relative smooth surface, semi-solid compact | 0.28 | 11 | 1.48 | 0.26 |
| Paracetamol–Magnesium Stearate | Extremely friable, loose compact | 0.23 | 10 | 0* | 0.22 |

* The occurrence of zero values is because these tablets are of such loose structures and the force required to break it is less than 0.6 kPa which is not covered in the detectable range or the used Schleuniger-2E used for strength measurement.

in column 3 were used for the comparative calculation of tablet strength based on Rumpf's theory, column 6.

The results show that the ranking of tablet strength follow the sequence as: Povidone > Crospovidone > Stearic Acid > Paracetamol > Pregelatinised Starch. Of the five Paracetamol tablets tested, three of them gave zero results (disregarded), and 2.03 kPa is the average of the two valid tests. The tablets of Pregelatinised Starch were very weak and only one out of the five tests was valid. The strength of binary-mixture tablets were all weaker than the compacts made from individual materials. The ranking sequence follows: Paracetamol–Stearic Acid > Paracetamol–Crospovidone > Paracetamol–Pregelatinised Starch > Paracetamol–Povidone > Paracetamol–Magnesium Stearate. Surprisingly, Paracetamol–Stearic Acid tablets showed the highest mechanical strength among the mixture compacts, higher than Paracetamol with Povidone or Pregelatinised Starch. It appears that neither Povidone nor Pregelatinised Starch exhibit binding functions towards Paracetamol crystals under dry condition.

Some general observations can be made from the experimental results of the interparticle van der Waals force and the compact strength. Pregelatinised Starch among the five individual substances has the lowest median adhesion force measured by AFM, and its strength as expected per Eq. (18) is the lowest. The fact that Povidone compact has the highest strength is due to its high plasticity and rather spherical shape which enables a large amount of surface area during compaction, evidenced by the SEM images of a pure Povidone compact (Fig. 7). Crospovidone has the highest median adhesion among the five materials according to AFM, and the compact does appear to hold together better than Stearic Acid and Paracetamol. Although Paracetamol has a similar median adhesion as Stearic Acid, its compact is weaker. Because Paracetamol particles have much higher elasticity than Stearic Acid particles, the available contact surface area between the constituent particles in the compact of Paracetamol is much less than in the compact of Stearic Acid, confirmed by SEM images in Fig. 8.

Although Povidone by itself forms very strong compact and Paracetamol also maintains some strength, their mixture makes a very weak tablet. This is caused by the fragile bonds between Paracetamol crystals and Povidone particles, where the median value of adhesion force under zero load was measured to be only 1.2 nN. For all the binary mixture tablets except Paracetamol–Magnesium Stearate: the strength of the mixture tablets is lower than for the tablets made of individual ingredients. Following the same pattern, the median adhesion forces between the pair particles of the binary mixtures are much lower than those between the pairs of the same kind (Table 4). An exception occurred in that Magnesium Stearate can be formed into a tablet with Paracetamol but not alone

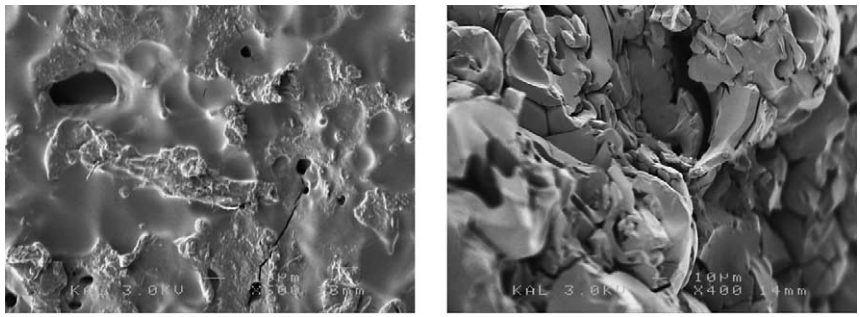

(a) (b)

Fig. 7. SEM images of a pure Povidone compact: (a) compact surface, (b) fracture surface.

under the same conditions. The explanation is that the 90% of Paracetamol in the binary mixture can still form the continuous phase and consequently maintain the structure. The 10% of Magnesium Stearate particles in the mixture is insufficient to eliminate all of the Paracetamol–Paracetamol bonds, although it does cause some interference and therefore affects the strength of the tablet.

The correlation between the median adhesion forces and the tablet strength is shown in Fig. 9. For all the binary pairs used here, it is the A–B type bond that is the weakest. Fig. 9 shows that the individual substance tablets and the binary mixture tablets all lie on the same straight line, except Povidone and Paracetamol–Magnesium Stearate. As discussed earlier, the pure Povidone tablet exhibits higher than expected strength due to its ductility, and the measured adhesion force between Magnesium Stearate and Paracetamol 100% is not reliable. The linear relationship is consistent with our simplistic derivation of tablet strength, Eq. (18). When all tablets are made under the same pressure and are of same mass, the average contact area increase $a/a'$, can be regarded as a constant if the mechanical properties of the materials are of the same order. From a statistical point of view, the number of contacts on a unit fracture plane, $n$, could also be regarded as a constant.

These results provide convincing evidence that the tablet strength is determined by the weakest bonds. When particles have the same order of adhesiveness, elasticity and plasticity dominates the compact strength through their significant impact on the contact surface area. When particles have the same order of elasticity and plasticity, it is the adhesiveness that is dominant.

This leads also to the conclusion that it is generally not feasible to use linear interpolation to describe yield pressure of binary mixture compacts from individual materials, for example (Newton and Cook, 1977), $\sigma_{mix} = \sigma_A\varphi_A + \sigma_B\varphi_B$, where $\varphi_A$ and $\varphi_B$ are the volume fractions of A and B, respectively.

Hypothetical tablet strengths were calculated using Rumpf's theory, Eq. (19). The porosity of the tablets

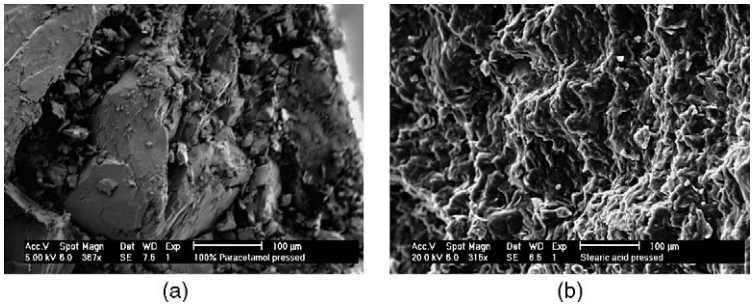


(a) (b)

Fig. 8. SEM images of (a) a pure Paracetamol compact and (b) a pure Stearic Acid compact.

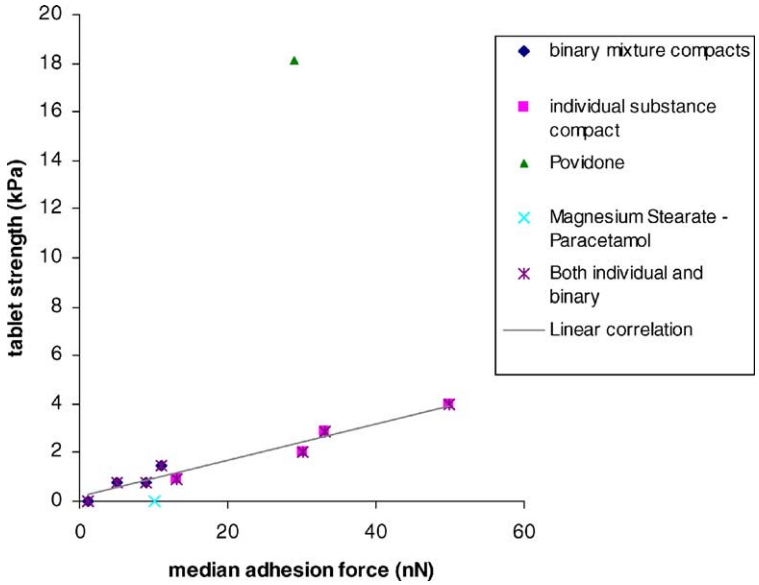


Fig. 9. The relationship between the inter-particle median adhesion force and the corresponding tablet strength.

were measured by pycnometry method; median adhesion forces measured from AFM were used for interparticle bonding force, and the coordination numbers were derived based on $k = (3.08/\varepsilon) - 1.13$ (van de Lagemaat et al., 2001). From the results in Table 4, it is apparent that most of the hypothetical tablet strengths using Rumpf's theory are three orders of magnitude smaller than the actual measured tablet strengths, and in the case of Povidone tablets it is four orders of magnitude less. If we accept the general structure of Rumpf's theory and extend it to compacted particle powder, it transpires that the interparticle bonding force in the compact should be about 1000 times the median adhesion force measured, or 10,000 times for Povidone. If the bonding force is attributed to van der Waals force only, this can be interpreted to suggest that the interparticle contact area has increased three orders after compaction (or four orders for Povidone). This needs to be experimentally verified, but seems highly plausible.

### 3.5. Flowability and compactibility

Particle flowability and compactibility, two properties which initially appear independent, are now shown as sharing almost the same mathematical functionality by comparing Eq. (15) with Eq. (18).

$$\rho_{\text{particle}} d^3 g \geq \frac{F_{\text{AFM}}}{\varepsilon} \frac{a}{a'} \tag{15}$$

$$\sigma = F_{\text{AFM}} n \frac{a}{a'} \tag{18}$$

The porosity $\varepsilon$ used in Eq. (15) has an equivalent implication as the number of contacts on a fracture plane $n$ in Eq. (18). Flowability and compactibility both reflect the strength of a particle aggregation, which is undesirable for particle flow but highly desired for compaction. Without altering contact surface energy, the most effective way to make a significant difference to the strength of a powder body is to change the effective contact surface area $a$. Increasing the strength can be implemented by reducing particle size, increasing size dispersion, reducing the elasticity, improving the plastic deformation, and moderating the surface roughness, amongst other methods. Promoting flowability would require the opposite changes. An ideal powder for pharmaceutical direct compaction at least should possess both good flowability and good compactibility, despite their contradictory property requirements. In this regard, finding an optimal balance is facilitated by the insights provided by the relationships exposed in Eqs. (15) and (18). Altering the

surface energy, elasticity and plasticity of the particles has been reflected in the practice of pharmaceutical particle design (Fachaux et al., 1995a, 1995b; Szabó-Révész et al., 2001), but our development permits a systematic, quantitative and theoretically informed approach.

## 4. Conclusions

The particle size, size distribution, morphology, adhesion force, flowability, and compactibility for six kinds of pharmaceutical materials have been examined and the inter-relations among them have been investigated. It is demonstrated that the pull-off adhesion force is a very important powder characterization parameter, particularly with regard to elucidating the causes of powder bulk properties, such as flowability and compactibility.

More specifically, a new model combining JKR theory and the surface roughness concept of Rumpf and Rabinovich is postulated for the interpretation and utilization of AFM measurement of the pull-off force between two irregularly shaped, roughly surfaced particles.

For particle flowability measurement, the application of tapping test and Hausner ratio has been reviewed experimentally and theoretically taking into account the interparticle adhesion force. The theory exposes why Hausner ratio is an unreliable flowability index. The particle rearrangement not only depends on the various particle properties, but also very much on the instantaneous energy supply from the tapping machine. For particles having high adhesiveness, or particles having very broad size distribution and irregular shape, Hausner ratio can be deceptive and misleading. A quantifiable flowability criterion based on fundamental properties of particles is developed and provided here.

In terms of particle compactibility, tablet strength is demonstrated to be determined by the weakest link. The compact strength is found theoretically and experimentally to have a direct correlation with the interparticle van der Waals force. When the particles are of similar elasticity and plasticity, the compact strength has a linear relationship with the interparticle adhesion force. Particle plasticity can be used to significantly alter the compact strength, exemplified by Povidone particles, by providing much greater interparticle contact area after compaction.

Particle flowability and compactibility are the two critical bulk properties in tabletting process. The lack of either is detrimental to the production. Particle flowability and compactibility are shown to share fundamental similarities, although the behavioral outcomes may be different depending on the dominating factors in particular different circumstances. The inter-relations demonstrated here serve to provide guidance in designing and synthesizing pharmaceutical and other particulate materials.

## Acknowledgements

This research is supported by Australian Research Council and Herron Pharmaceuticals Ltd. We acknowledge the following technical support: Ms Maribel De La Garza, Technical University of Munich; Mr. David Page, University of Queensland; Paul Martell and Darren Teng, undergraduate students from Chemical Engineering, University of Queensland for conducting various measurements involved in this work; Mr. Nicholas Woods and Mr. Gary Dorr for access and assistance with Malvern 2600.

## References

Abdullah, E.C., Geldart, D., 1999. The use of bulk density measurements as flowability indicators. Powder Technol. 102, 151–165.

Alderborn, G., 1996. Particle dimensions. In: Nystrom, C. (Ed.), Pharmaceutical Powder Compaction Technology. Marcel Dekker, Inc., New York, pp. 245–282.

Beach, E.R., Tormoen, G.W., Drelich, J., Han, R., 2002. Pull-off force measurements between rough surfaces by atomic force microscopy. J. Colloid Interface Sci. 247, 84–99.

Beyer, T., Day, G.M., Price, S.L., 2001. The prediction, morphology, and mechanical properties of the polymorphs of paracetamol. J. Am. Chem. Soc. 123, 5086–5094.

Bolhuis, G.K., Chowhan, Z.T., 1996. Materials for direct compaction. In: Nystrom, C. (Ed.), Pharmaceutical Powder Compaction Technology. Marcel Dekker, Inc., pp. 419–500.

Davies, P.N., Newton, J.M., 1996. Mechanical strength. In: Nystrom, C. (Ed.), Pharmaceutical Powder Compaction Technology. Marcel Dekker, New York, pp. 165–191.

Derjaguin, B.V., Abrikosova, I.I., Lifshitz, E.M., 1956. Q. Rev. Chem. Soc. 10, 295.

Fachaux, J.M., Guyot-Hermann, A.M., Guyot, J.C., Conflant, P., Drache, M., Veesler, S., Boistelle, R., 1995a. Pure Paracetamol

for direct compression: part I. Development of sintered-like crystals of Paracetamol. Powder Technol. 82, 123–128.
Fachaux, J.M., Guyot-Hermann, A.M., Guyot, J.C., Conflant, P., Drache, M., Veesler, S., Boistelle, R., 1995b. Pure Paracetamol for direct compression: part II. Study of the physicochemical and mechanical properties of sintered-like crystals of Paracetamol. Powder Technol. 82, 129–133.
Fuhrer, C., 1996. Interparticulate attraction mechanisms. In: Nystrom, C. (Ed.), Pharmaceutical Powder Compaction Techology. Marcel Dekker, Inc., New York.
Garekani, H.A., Ford, J.L., Rubinstein, M.H., Rajabi-Siahboomi, A.R., 2000. Highly compressible paracetamol: I: crystallization and characterization. Int. J. Pharm. 208, 87–89.
Geldart, D., Harnby, N., Wong, A.C., 1984. Fluidization of cohesive powders. Powder Technol. 37, 25–37.
Geldart, D., Wong, A.C.Y., 1984. Fluidization of powders showing degrees of cohesiveness: I. Bed expansion. Chem. Eng. Sci. 39, 1481–1488.
Gotzinger, M., Peukert, W., 2003. Dispersive forces of particle-surface interactions: direct AFM measurements and modelling. Powder Technol. 130, 102–109.
Guerin, E., Tchoreloff, P., Leclerc, B., Tanguy, D., Deleuil, M., Couarraze, G., 1999. Rheological characterization of pharmaceutical powders using tap testing, shear cell and mercury porosimeter. Int. J. Pharm. 189, 91–103.
Hiestand, E.N., 1985. Dispersion forces and plastic deformation in tablet bond. J. Pharm. Sci. 74, 768–770.
Hiestand, E.N., 1991. Tablet bond: I. A theoretical model. Int. J. Pharm. 67, 217–229.
Jivraj, M., Martini, L.G., Thomson, C.M., 2000. An overview of the different excipients useful for the direct compression of tablets. Pharm. Sci. Technol. Today 3, 58–63.
Johnson, K.L., Kendall, K., Roberts, A.D., 1971. Surface energy and the contact of elastic solids. Proc. R. Soc. Lond. A. 324, 301–313.
Kawakita, K., Ludde, K.-H., 1970. Some considerations on powder compression equations, Powder Technol., 61–68.
Kibbe, A.H., 2000. Handbook of Pharmaceutical Excipients. Pharmaceutical press.
Krupp, H., 1967. Particle adhesion theory and experiment. Adv. Colloid Interface Sci. 1, 111–239.
Leuenberger, H., 1982. The compressibility and compactibility of powder systems. Int. J. Pharm. 12, 41–55.
Martino, P.D., Guyot-Hermann, A.-M., Conflant, P., Drache, P., Guyot, J.-C., 1996. A new pure Paracetamol for direct compression: the orthorhombic form. Int. J. Pharm. 128, 1–8.
Molerus, O., 1982. Interpretation of Geldart's type A, B, C and D powders by taking into account interparticle cohesion forces. Powder Technol. 33, 81–87.
Muzzio, F.J., Shinbrot, T., Glasser, B.J., 2002. Powder technology in the pharmaceutical industry: the need to catch up fast. Powder Technol. 124, 1–7.
Newton, J.M., Cook, D.T., 1977. The strength of tablets of mixed components. J. Pharm. Pharmacol. 29, 247–249.
Podczeck, F., Newton, J.M., James, M.B., 1997. Variations in the adhesion force between a drug and carrier particles as a result of changes in the relative humidity of the air. Int. J. Pharm. 149, 151–160.
Quintanilla, M.A.S., Castellanos, A., Valverde, J.M., 2001. Correlation between bulk stresses and interparticle cotnact forces in fine powders. Phys. Rev. E. 64, 031301(1–9).
Rabinovich, Y.I., Adler, J.J., Ata, A., Singh, R.K., Moudgil, B.M., 2000a. Adhesion between nanoscale rough surfaces I. role of asperity geometry. J. Colloid Interface Sci. 232, 10–16.
Rabinovich, Y.I., Adler, J.J., Ata, A., Singh, R.K., Moudgil, B.M., 2000b. Adhesion between nanoscale rough surfaces II. measurement and comparison with theory. J. Colloid Interface Sci. 232, 17–24.
Rumpf, H., 1962. In: Knepper, W.A. (Ed.), Agglomeration. Interscience, New York, pp. 379.
Rumpf, H., 1970. Zur Theorie der Zugfestigkeit von Agglomeraten bei Kraftübertragung an Kontaktpunkten. Chemie-Ing. Technik, 538.
Rumpf, H., 1990. Particle Technology. London, Chapman & Hall.
Schussele, A., Bauer-Brandl, A., 2003. Note on the mesaurement of flowability according to the European Pharmacopoeia. Int. J. Pharm. 257, 301–304.
Staniforth, J., 2002. Powder flow. In: Aulton, M.E. (Ed.), Pharmaceutics: The Science of Dosage Form Design. Churchill Livingstone, pp. 197–210.
Szabó-Révész, P., Göczõ, H., Pintye-Hódi, Kásajr, P., Erõs, I., Hasznos-Nezdei, M., Farkas, B., 2001. Development of spherical crystal agglomerates of an aspartic acid salt for direct tablet making, Powder Technol. 114, 118–124.
van de Lagemaat, J., Benkstein, K.D., Frank, A.J., 2001. Relation between particle coordination number and porosity in nanoparticle films: implications to dye-sensitized solar cells. J. Phys. Chem. B 105, 12433–12436.
van Veen, B., Maarschalk, K.V.D.V., Bolhuis, G.K., Zuurman, K., Frijlink, H.W., 2000. Tensile strength of tablets containing two materials with a different compaction behaviour. Int. J. Pharm. 203, 71–79.
Yu, A.B., Hall, J.S., 1994. Packing of fine powders subjected to tapping. Powder Technol. 78, 247–256.
Zenz, F.A., Othmer, D.F., 1960. Fluidization and Fluid-Particle Systems. New York, Reinhold Publishing Corporation.